Inorg. Chem. **2005**, *44*, 2159–2168

Reactions of Laser-Ablated Uranium Atoms with H_2O in Excess Argon: A Matrix Infrared and Relativistic DFT Investigation of Uranium Oxyhydrides

Binyong Liang, Rodney D. Hunt,[†] Gary P. Kushto,[‡] and Lester Andrews*

Department of Chemistry, University of Virginia, P.O. Box 400319, Charlottesville, Virginia 22904-4319

Jun Li*

William R. Wiley Environmental Molecular Sciences Laboratory, Pacific Northwest National Laboratory, Richland, Washington 99352

Bruce E. Bursten*

Department of Chemistry, The Ohio State University, Columbus, Ohio 43210

Received November 15, 2004

Laser-ablated U atoms react with H_2O during condensation in excess argon. Infrared absorptions at 1416.3, 1377.1, and 859.4 cm^{-1} are assigned to symmetric H—U—H, antisymmetric H—U—H, and U═O stretching vibrations of the primary reaction product H_2UO. Uranium monoxide, UO, also formed in the reaction, inserts into H_2O to produce HUO(OH), which absorbs at 1370.5, 834.3, and 575.7 cm^{-1}. The HUO(OH) uranium(IV) product undergoes ultraviolet photoisomerization to a more stable H_2UO_2 uranium(VI) molecule, which absorbs at 1406.4 and 885.9 cm^{-1}. Several of these species, particularly H_2UO_2, appear to form weak Ar-coordinated complexes. The predicted vibrational frequencies, relative absorption intensities, and isotopic shifts from relativistic DFT calculations are in good agreement with observed spectra, which further supports the identification of novel uranium oxyhydrides from matrix infrared spectra.

I. Introduction

The chemistry of uranium, particularly the hydrolysis reaction, is of major importance in the design of nuclear waste repositories and nuclear fuel reprocessing cycles.[1,2] Uranium reactions with water have been studied extensively. In particular, studies have focused on the corrosive effect of steam on uranium fuel elements, which is a major safety concern in the operation of nuclear fission reactors.[3−5] Other investigations have examined the kinetics of the uranium reaction with water vapor in the presence of oxygen and/or hydrogen.[6−11] It was found that water acts as a catalyst for uranium corrosion in humid air, especially at higher temperatures.[11] The reaction of uranium with water vapor produces binary oxides with concomitant formation of H_2, as described by the following general equation:

$$U + xH_2O \rightarrow UO_x + xH_2$$

Values of the O/U ratio (x) of the oxide product vary from

* Authors to whom correspondence should be addressed. E-mail: lsa@virginia.edu (L.A.); jun.li@pnl.gov (J.L.); bursten.l@osu.edu (B.E.B).
† Guest worker from Chemical Technology Division, Oak Ridge National Laboratory, Oak Ridge, TN 37831-6273.
‡ Present address: Optical Sciences Branch, United States Naval Research Laboratory, Washington, DC 10375.

(1) Engkvist, I.; Albinsson, Y. *Radiochim. Acta* **1992**, *58/59*, 109.
(2) Erten, H. N.; Mohammed, A. K.; Choppin, G. R. *Radiochim. Acta* **1994**, *66/67*, 123.
(3) Hopkinson, B. E. *J. Electrochem. Soc.* **1959**, *106*, 102.
(4) Cerrai, E.; Scaroni, A. *J. Nucl. Mater.* **1968**, *27*, 264.
(5) Krikorian, O. H. *High Temp.−High Pressures* **1982**, *14*, 387.
(6) Magnani, N. M. *Sandia Natl. Lab. [Tech. Rep.] SAND* **1974**, SAND-74−0145.
(7) Jackson, R. L.; Condon, J. B.; Steckel, L. M. *Union Carbide Corp., [Nucl. Div.], Oak Ridge Y-12 Plant, [Tech. Rep.] Y* **1977**, Y-2028.
(8) Ritchie, A. G. *J. Nucl. Mater.* **1981**, *102*, 170.
(9) Ritchie, A. G.; Greenwood, R. C.; Randles, S. J. *J. Nucl. Mater.* **1986**, *139*, 121.
(10) Balooch, M.; Hamza, A. V. *J. Nucl. Mater.* **1996**, *230*, 259.
(11) Haschke, J. M. *J. Alloys Compd.* **1998**, *278*, 149.

10.1021/ic0483951 CCC: $30.25
Published on Web 03/04/2005

2.0 to 2.2, depending on temperature and water pressure.[6,12] However, little is known about the intermediates and the mechanisms of the important gas-phase reaction between uranium and water.

Because laser ablation can overcome the extreme refractory nature of uranium and provide atomic vapor, this method has been used in recent studies of reactions between uranium atoms and small molecules.[13−23] Although reactions between actinide metal atoms and water molecules are represented by one study involving thorium,[24] the reactions of beryllium,[25] the boron family,[26,27] and the transition metal atoms[28−32] with water have been investigated using both thermal and laser-ablation methods. There are also recent studies on the aqueous Th(IV) species and molecular dynamic simulations on Th(IV) hydrates in aqueous solutions.[33,34] Here we present a matrix infrared spectroscopic study of the reactions of laser-ablated uranium atoms with water molecules. Additionally, relativistic DFT calculations were performed to support the spectroscopic assignments and to elucidate the bonding and electronic structures of the novel reaction products.

II. Experimental and Computational Section

The experimental method for laser ablation and matrix isolation has been described in detail previously.[35−37] Briefly, the Nd:YAG laser fundamental (1064 nm, 10 Hz repetition rate with 10 ns pulse width, 3−5 mJ/pulse) was focused onto the rotating uranium metal target (Oak Ridge National Laboratory). Laser-ablated metal atoms were codeposited with H_2O (0.05%−0.5%) in excess argon onto a 7 K CsI cryogenic window at 2−4 mmol/h for 1−1.5 h. Distilled H_2O, D_2O, and $H_2{}^{18}O$ were evaporated from separate $^1/_4$ in. Swagelok fingers through Nupro fine-metering valves into the argon stream. Additional experiments were also performed on laser-ablated U atoms reacting with H_2 (1−2%) and O_2 (0.1%) mixtures. Fourier transform infrared spectra were recorded at 0.5 cm^{-1} resolution on a Nicolet 550 spectrometer with 0.1 cm^{-1} accuracy using a mercury cadmium telluride detector down to 400 cm^{-1}. Matrix samples were annealed at different temperatures, and selected samples were subjected to irradiation using a medium-pressure mercury lamp ($\lambda > 240$ nm) with the globe removed and optical filters applied when needed.

Density functional theoretical calculations were performed by using the Amsterdam density functional (ADF 2.3) code.[38] The gradient-corrected exchange-correlation functional of Perdew and Wang (PW91) was used.[39,40] Scalar relativistic effects were taken into account by using quasi-relativistic Pauli formalism[41] and the zero-order regular approximation (ZORA).[42] The $1s^2$ core for O, $1s^22p^6$ core for Ar, and $1s^25d^{10}$ core for U were treated via the frozen core approximation.[43] Uncontracted Slater-type-orbital (STO) basis sets of triple-ζ quality were used for the valence orbitals of U, O, H, and Ar, with d- and f-type polarization functions for O and Ar atoms and p- and d-type polarization functions for H atoms.[44] All geometries were fully optimized with the inclusion of scalar relativistic effects. Vibrational frequencies and infrared intensities were determined via numerical evaluation of the second-order derivatives of the total energies. Since some of these transient species have very soft vibrational modes, numerical integration accuracy of INTEGRATION = 10.0 was used throughout, together with very tight convergence criteria for energy iterations and for geometry optimizations. Further computational details have been described elsewhere.[45] All the calculations were performed using the supercomputers at the molecular science computing facilities (MSCF) at the William R. Wiley Environmental Molecular Sciences Laboratory.

III. Results and Discussion

Product absorptions from the U/H_2O and $U/H_2/O_2$ reactions will be identified with the support of DFT calculations. Over 40 matrix isolation experiments were performed to find the optimum laser energy and water concentration for new product absorptions.

A. U + H_2O. Infrared spectra of the matrix-isolated products from the reaction of uranium atoms and H_2O are shown in Figure 1, and the various isotopic spectra are shown

(12) Colmenares, C. A. *J. Solid State Chem.* **1984**, *15*, 257.
(13) Gibson, J. K. *J. Mass Spectrom.* **1999**, *34*, 1166.
(14) Zhou, M. F.; Andrews, L.; Li, J.; Bursten, B. E. *J. Am. Chem. Soc.* **1999**, *121*, 9712.
(15) Andrews, L.; Liang, B.; Li, J.; Bursten, B. E. *Angew. Chem., Int. Ed.* **2000**, *39*, 4565.
(16) Liang, B.; Andrews, L.; Li, J.; Bursten, B. E. *J. Am. Chem. Soc.* **2002**, *124*, 9016.
(17) Andrews, L.; Liang, B.; Li, J.; Bursten, B. E. *J. Am. Chem. Soc.* **2003**, *125*, 3126.
(18) Liang, B.; Andrews, L.; Li, J.; Bursten, B. E. *Chem.−Eur. J.* **2003**, *9*, 4781.
(19) Liang, B.; Andrews, L.; Li, J.; Bursten, B. E. *Inorg. Chem.* **2004**, *43*, 882.
(20) Zhou, M. F.; Andrews, L.; Ismail, N.; Marsden, C. *J. Phys. Chem. A* **2000**, *104*, 5495.
(21) Heinemann, C.; Schwarz, H. *Chem.−Eur. J.* **1995**, *1*, 7.
(22) Marcalo, J.; Leal, J. P.; deMatos, A. P.; Marshall, A. G. *Organometallics* **1997**, *16*, 4581.
(23) (a) Hunt, R. D.; Andrews, L. *J. Chem. Phys.* **1993**, *98*, 3690. (b) Hunt, R. D.; Yustein, J. T.; Andrews, L. *J. Chem. Phys.* **1993**, *98*, 6070.
(24) Liang, B.; Andrews, L.; Li, J.; Bursten, B. E. *J. Am. Chem. Soc.* **2002**, *124*, 6723 (Th+H_2O).
(25) Thompson, C. A.; Andrews, L. *J. Phys. Chem.* **1996**, *100*, 12214.
(26) Hauge, R. H.; Kauffman, J. W.; Margrave, J. L. *J. Am. Chem. Soc.* **1980**, *102*, 6005.
(27) Andrews, L.; Burkholder, T. R. *J. Phys. Chem.* **1991**, *95*, 8554.
(28) Kauffman, J. W.; Hauge, R. H.; Margrave, J. L. *J. Phys. Chem.* **1985**, *89*, 3541, 3547.
(29) Zhang, L. N.; Dong, J.; Zhou, M. F. *J. Phys. Chem. A* **2000**, *104*, 8882.
(30) Zhou, M. F.; Zhang, L. N.; Dong, J.; Qin, Q. Z. *J. Am. Chem. Soc.* **2000**, *122*, 10680.
(31) Zhou, M. F.; Dong, J.; Zhang, L. N.; Qin, Q. Z. *J. Am. Chem. Soc.* **2001**, *123*, 135.
(32) Zhang, L. N.; Zhou, M. F.; Shao, L. M.; Wang, W. N.; Fan, K. N.; Qin, Q. Z. *J. Phys. Chem. A* **2001**, *105*, 6998.
(33) Rothe, J.; Denecke, M. A.; Neck, V.; Muller, R.; Kim, J. I. *Inorg. Chem.* **2002**, *41*, 249.
(34) Yang, T.; Tsushima, S.; Suzuki, A. *J. Phys. Chem. A.* **2001**, *105*, 10439.
(35) Burkholder, T. R.; Andrews, L. *J. Chem. Phys.* **1991**, *95*, 8697.
(36) Hassanzadeh, P.; Andrews, L. *J. Phys. Chem.* **1992**, *96*, 9177.
(37) Chertihin, G. V.; Saffel, W.; Yustein, J. T.; Andrews, L.; Neurock, M.; Ricca, A.; Bauschlicher, C. W., Jr. *J. Phys. Chem.* **1996**, *100*, 5261.
(38) ADF 2.3, Theoretical Chemistry, Vrije Universiteit, Amsterdam, referenced in: (a) Baerends, E. J.; Ellis, D. E.; Ros, P. *Chem. Phys.* **1973**, *2*, 42. (b) te Velde, G.; Baerends, E. J. *J. Comput. Phys.* **1992**, *99*, 94. (c) Fonseca Guerra, C.; Visser, O.; Snijders, J. G.; te Velde, G.; Baerends, E. J. In *Methods and Techniques for Computational Chemistry*; Clementi, E., Corongiu, G., Eds.; STEF: Cagliari, Italy, 1995; p 305.
(39) Perdew, J. P.; Wang, Y. *Phys. Rev. B* **1992**, *45*, 13244.
(40) Perdew, J. P.; Chevary, J. A.; Vosko, S. H.; Jackson, K. A.; Peterson, M. R.; Singh, D. J.; Foilhais, C. *Phys. Rev. B* **1992**, *46*, 6671.
(41) Ziegler, T.; Baerends, E. J.; Snijders, J. G.; Ravenek, W. *J. Phys. Chem.* **1989**, *93*, 3050.
(42) van Lenthe, E.; Baerends, E. J.; Snijders, J. G. *J. Chem. Phys.* **1993**, *99*, 4597.
(43) Baerends, E. J.; Ellis, D. E.; Ros, P. *Chem. Phys.* **1973**, *2*, 42.
(44) van Lenthe, E.; Baerends, E. J. *J. Comput. Chem.* **2003**, *24*, 1142.
(45) Li, J.; Bursten, B. E. *J. Am. Chem. Soc.* **1997**, *119*, 9021.

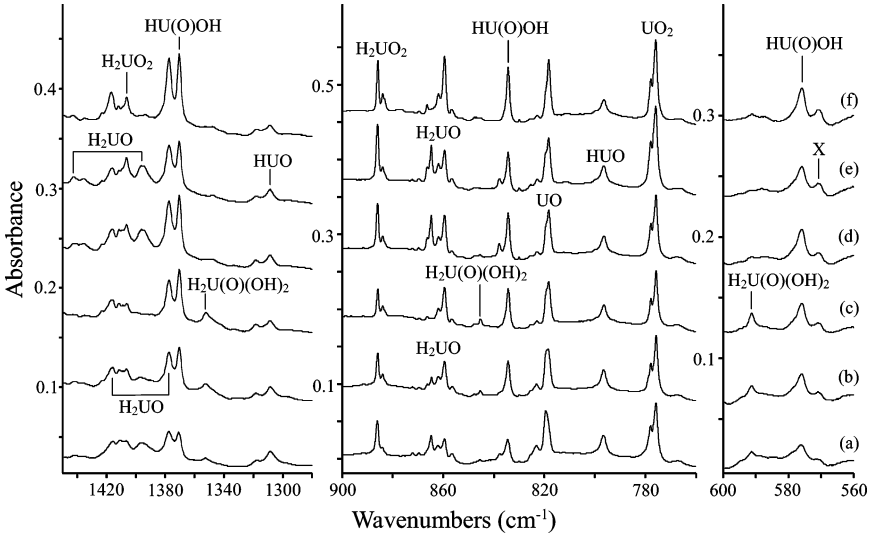

Figure 1. Infrared spectra in the 1450−1280, 900−760, and 600−560 cm^{-1} regions for laser-ablated U codeposited with 0.2% H_2O in argon at 7 K. (a) Sample deposited for 70 min, (b) after 25 K annealing, (c) after 30 K annealing, (d) after $\lambda > 290$ nm irradiation, (e) after $\lambda > 240$ nm irradiation, and (f) after 35 K annealing.

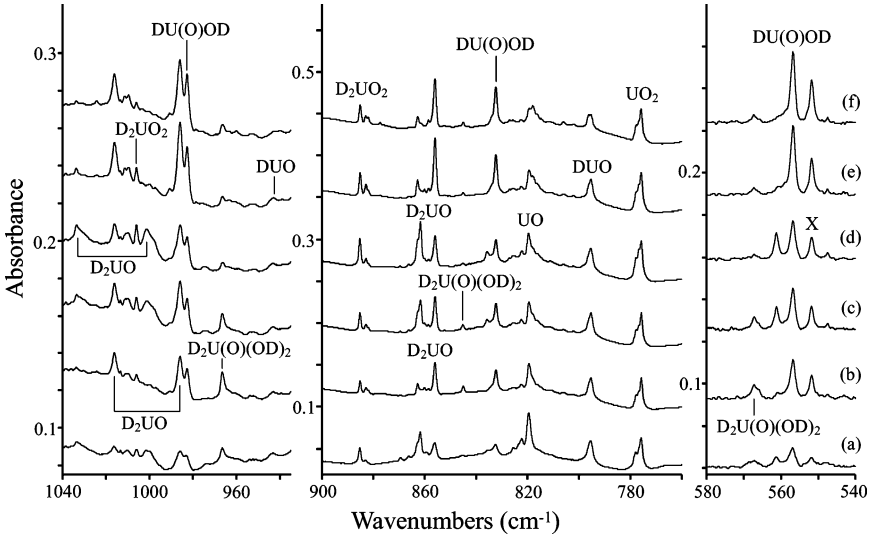

Figure 2. Infrared spectra in the 1040−935, 900−760, and 580−540 cm^{-1} regions for laser-ablated U codeposited with 0.15% D_2O in argon at 7 K. (a) Sample deposited for 70 min, (b) after 30 K annealing, (c) after $\lambda > 380$ nm irradiation, (d) after $\lambda > 240$ nm irradiation, (e) after 35 K annealing, and (f) after 40 K annealing.

in Figures 2−4. Frequencies of the observed bands and their isotopic counterparts, along with their proposed assignments, are listed in Table 1. The computationally optimized geometry parameters of various species are listed in Table 2, and the geometry structures of several important species are depicted in Figure 5. The uranium oxides UO (819.7 cm^{-1}) and UO_2 (775.9 cm^{-1}) are major reaction products, and very weak UH_4 (1483.6 cm^{-1}) and UH (1423.7 cm^{-1}) bands are identified from previous work.[23a,46,47] In this experiment, hydride bands showed no ^{18}O isotopic shifts, and not surprisingly, oxide bands showed no deuterium shifts. In a typical experiment, the UH band intensities are less than 10% of the 1377.1 cm^{-1} H_2UO band and UH_4 is too weak to be observed. Product bands also included Ar_nH^+ at 903.6 cm^{-1}, Ar_nD^+ at 643.1 cm^{-1},[48] and HO_2 and DO_2 at 1388.4 and 1019.8 cm^{-1}, respectively.[49] No evidence was found for a U—OH_2 complex in the 1500−1700 cm^{-1} region. The 1051.0 cm^{-1} absorption[23b] of UN_2 was not observed, indicating no significant air leak.

1. H_2UO. The 859.4 cm^{-1} band observed after deposition was favored by annealing, and the intensity doubled on 30 K annealing. It showed little change on the following two irradiations and then increased again on 35 K annealing. The 859.4 cm^{-1} band in the U═O stretching region red-shifted to 813.9 cm^{-1} in the $H_2{}^{18}O$ experiment. The $^{16}O/^{18}O$ isotopic frequency ratio of 1.0559 is slightly smaller than the diatomic UO value of 1.0569. In the mixed $H_2{}^{16}O + H_2{}^{18}O$ experiment, only a doublet with two pure isotopic bands was

(46) Gabelnick, S. D.; Reedy, G. T.; Chasanov, M. G. *J. Chem. Phys.* **1973**, *58*, 4468.
(47) Souter, P. F.; Kushto, G. P.; Andrews, L.; Neurock, M. *J. Am. Chem. Soc.* **1997**, *119*, 1682.
(48) (a) Milligan, D. E.; Jacox, M. E. *J. Mol. Spectrosc.* **1973**, *46*, 460. (b) Wight, C. A.; Ault, B. S.; Andrews, L. *J. Chem. Phys.* **1976**, *65*, 1244.
(49) Milligan, D. E.; Jacox, M. E. *J. Chem. Phys.* **1963**, *38*, 2627. Smith, D. W.; Andrews, L. *J. Chem. Phys.* **1974**, *60*, 81.

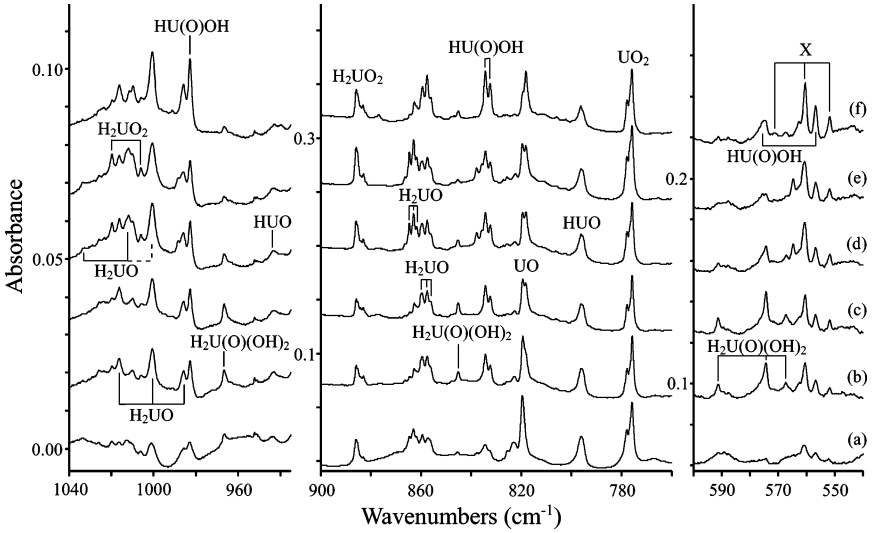

Figure 3. Infrared spectra in the 1040−935, 900−760, and 600−540 cm^{-1} regions for laser-ablated U codeposited with 0.16% H_2O + 0.21% HDO + 0.07% D_2O in argon at 7 K. (a) Sample deposited for 80 min, (b) after 30 K annealing, (c) after 35 K annealing, (d) after $\lambda > 290$ nm irradiation, (e) after $\lambda > 240$ nm irradiation, and (f) after 40 K annealing.

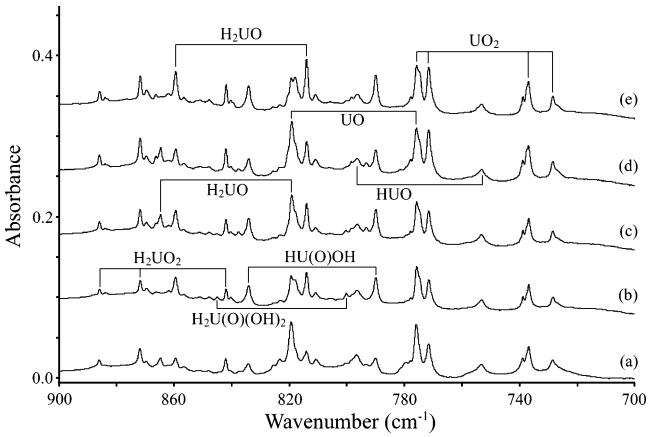

Figure 4. Infrared spectra in the 900−700 cm^{-1} regions for laser-ablated U codeposited with 0.10% H_2O + 0.12% $H_2{}^{18}O$ in argon at 7 K. (a) Sample deposited for 100 min, (b) after 30 K annealing, (c) after $\lambda > 380$ nm irradiation, (d) after $\lambda > 240$ nm irradiation, and (e) after 35 K annealing.

observed. In the D_2O experiment, this band shifted to 856.0 cm^{-1}; it is clear that this band is due to a H-perturbed U═O vibration. Other decisive evidence comes from the mixed H_2O + HDO + D_2O (H/D molar ratio about 1.5:1) experiment: this band showed a triplet feature with a new 857.5 cm^{-1} band between the two pure isotopic bands (Figure 3). The 859.4 cm^{-1} band is assigned as a U═O vibrational mode perturbed by two *equivalent* hydrogen atoms. We note that the U—O stretching frequency in U(IV) H_2UO is higher than that in U(II) UO, consistent with the higher formal oxidation state of U in the former complex.

In the U—H vibrational region around 1400 cm^{-1}, two bands at 1416.3 and 1377.1 cm^{-1} tracked with the 859.4 cm^{-1} band throughout all experiments. After 35 K annealing (where the bands have the highest absorptions), the integrated areas of these three bands (1416.3, 1377.1, and 859.4 cm^{-1}) are 0.143, 0.330, and 0.136 AU (absorbance units) cm^{-1}, respectively. The 1416.3 cm^{-1} band red-shifted to 1016.2 cm^{-1} in the D_2O experiment, and no shift was observed with $H_2{}^{18}O$. The 1377.1 cm^{-1} band red-shifted to 986.0 cm^{-1} with D_2O and to 1376.9 cm^{-1} with $H_2{}^{18}O$. On the basis of the relative intensities and isotopic data, the 1416.3 and 1377.1 cm^{-1} bands are assigned, respectively, as the symmetric and antisymmetric stretching vibrations in a H—U—H unit. These assignments are also supported by the mixed H_2O + HDO + D_2O experiment, where a new band at 1000.7 cm^{-1} tracked with the above bands and gave a 1016.2, 1000.7, 986.0 cm^{-1} triplet (Figure 3). The 1000.7 cm^{-1} band is only 0.4 cm^{-1} lower than the median of the 1016.2 and 986.0 cm^{-1} bands, which are the deuterium counterparts of the 1416.3 and 1377.1 cm^{-1} bands. This new band is assigned to the U—D stretching vibration in a H—U—D unit, where nearly no interaction is present between U—H and U—D modes because of the huge mass difference of H and D atoms. The U—H stretching vibration in the same H—U—D unit cannot

Table 1: Infrared Absorptions (cm^{-1}) of Reaction Products from Laser-Ablated U Atoms with H_2O in Excess Argon

H_2O	$H_2{}^{18}O$	D_2O	assignment
1442.7	1441.9	1033.6	H_2UO site
1435.3	1435.3		UH site
1423.7	1423.7		UH
1416.3	1416.3	1016.2	H_2UO
1406.4	1406.3	1006.0	H_2UO_2
1396.3	1395.4	1001.3	H_2UO site
1377.1	1376.9	986.0	H_2UO
1370.5	1370.3	982.7	HUO(OH)
1352.3	1352.5	966.6	$H_2UO(OH)_2$
1308.2	1308.2	932.5	(HUO)
903.4	903.4	643.3	Ar_nH^+
885.9	842.0	885.2	H_2UO_2
884.0	840.3	882.8	H_2UO_2 site
864.8	819.4	861.6	H_2UO site
859.4	813.9	856.0	H_2UO
856.8	811.1		H_2UO site
845.3	800.2	845.1	$H_2UO(OH)_2$
837.8	793.2	835.7	HUO(OH) site
834.3	789.9	832.3	HUO(OH)
819.7	775.6	819.6	UO
818.2	774.5	818.1	UO site
796.5	753.2	795.4	(HUO)
777.9	738.8	777.9	UO_2 site
775.9	736.8	775.8	UO_2
591.2	566.2	567.3	$H_2UO(OH)_2$
575.7		556.8	HUO(OH)
570.5		551.8	X

Table 2: Ground Electronic States, Equilibrium Geometries, and Isotopic Frequencies Calculated for the U + H_2O Reaction Products

species	state sym	geometry (Å, deg)		frequencies (intensity)
HUO	$^4A''$, C_s	U—H: 1.992, U═O: 1.823; ∠HUO: 105.6	H—^{16}O	301(66), 862(218), 1443(389)
			D—^{16}O	220, 861, 1024
			H—^{18}O	300, 816, 1442
H_2UO	$^3A''$, C_s	U—H: 1.987, U═O: 1.813; ∠OUH: 93.0, ∠HUH: 99.4	H—^{16}O	318(15), 366(126), 503(40), 871(215), 1428(618), 1485(543)
			D—^{16}O	235, 269, 358, 868, 1013, 1057
			H—^{18}O	317, 365, 503, 825, 1428, 1485
HU(O′)(OH)	^3A, C_1	U—H: 1.997, U═O′: 1.831, U—O: 2.034, O—H: 0.965; ∠HUO′: 100.3, ∠HUO: 96.3, ∠OUO′: 103.2, ∠UOH: 159.2	H—^{16}O	133(9), 272(59), 344(113), 380(104), 393(98), 625(171), 854(266), 1457(417), 3805(180)
			D—^{16}O	124, 200, 246, 299, 301, 604, 853, 1034, 2773
			H—^{18}O	127, 270, 344, 376, 390, 596, 808, 1457, 3792
H_2UO_2	^1A_g, D_{2h}	U—H: 2.009, U═O: 1.796,	H—^{16}O	130(26), 200(7), 207(242), 45(0), 558(22), 848(0), 943(422), 1408(687), 1435(0)
			D—^{16}O	127, 203, 210, 345, 453, 845, 940, 987, 1037
			H—^{18}O	120, 193, 295, 469, 633, 805, 899, 1389, 1451
$H_2U(O')(OH)_2$	$^1A'$, C_s	U—H: 1.966, U═O′: 1.809, U—O: 2.029, O—H: 0.966; ∠HUO′: 89.5, ∠HUH: 173.5, ∠OUO: 94.2	H—^{16}O	114(16), 130(5), 143(31), 205(78), 282(60), 287(82), 329(119), 344(60), 461(6), 493(38), 561(6), 637(197), 661(128), 869(243), 1445(606), 1470(3), 3773(230), 3800(217)
			D—^{16}O	105, 114, 119, 167, 200, 235, 267, 275, 339, 358, 416, 590, 632, 862, 1027, 1045, 2749, 2770
			H—^{18}O	109, 125, 138, 202, 281, 282, 322, 340, 459, 488, 548, 619, 635, 825, 1445, 1470, 3760, 3787

be observed due to the strong HDO absorptions in the region. On the basis of the above experimental evidence, the novel H_2UO molecule is identified.

Relativistic DFT calculations on H_2UO predict a C_s symmetry, $^3A''$ ground-state pyramidal structure (Figure 5a) with the following metric parameters: U═O = 1.813 Å, U—H = 1.987 Å, ∠HUH = 99.4°, and ∠OUH = 93.0°. The degree of pyramidalization of the molecule can be gauged by the dihedral angle of the HUH and OUX planes, χ = O—U—X, where X is the midpoint of the two H atoms. For a planar molecule, such as H_2CO, $\chi = 180°$. For H_2UO, $\chi = 94.7°$, indicative of the high degree of pyramidalization at the U atom, as was the case in our previous study of H_2ThO ($\chi = 107.6°$).[24] This structure is found to be much more stable than its U(II) isomer HU(OH); the triplet and the quintet states of the latter are found to be 30.5 and 32.6 kcal/mol higher in energy than the H_2UO ground state. The vibrational analysis of H_2UO predicts three modes at 1485 cm^{-1} (predominantly H—U—H symmetric stretch), 1428 cm^{-1} (H—U—H antisymmetric stretch), and 871 cm^{-1} (U—O stretch) with infrared intensities of 543, 618, and 215 km/mol, respectively. The calculated frequencies for the free H_2UO molecule are slightly too high, due to the neglect of the expected weak U—Ar interaction in an Ar matrix (see below) and the expected inaccuracy of the DFT method used. Nonetheless, the calculated frequencies still fit the experimental values reasonably well, with scaling factors of 0.954, 0.964, and 0.986, respectively. The relative intensities also follow the observed trend, except for an overestimation of the symmetric UH_2 mode. Several higher symmetry C_{2v} H_2UO states were also calculated, with the lowest triplet being some 5 kcal/mol higher than the $^3A''$ ground state. Without including spin—orbit coupling, the triplet ground state is expected for these U(IV) H_2UO species, which have f^2 electron configurations.

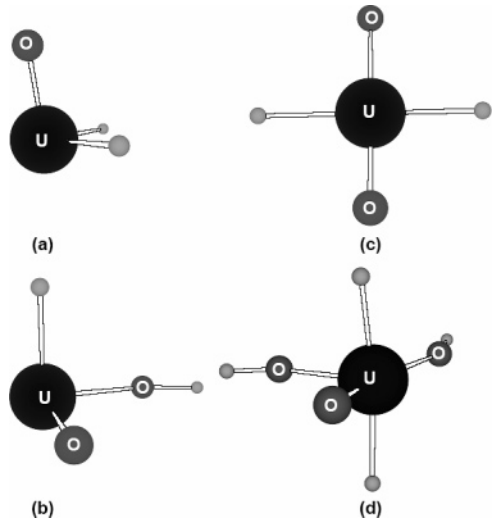

Figure 5. Optimized lowest-energy geometry structures of (a) H_2UO, (b) HUO(OH), (c) H_2UO_2, and (d) $H_2UO(OH)_2$. The H atoms are not labeled for clarity.

As in the case of H_2ThO, the pyramidal structure of H_2UO allows for the more effective use of both the U 5f and 6d orbitals in the bonding of the H and O atoms. The pyramidal structure also leaves the U atom available for the coordination of additional ligands that might be available. In particular, we have recently shown that U(VI), U(V), and U(IV) species such as CUO, UO_2^+, and UO_2 can be stabilized by the formation of direct U—Ar bonds.[50−52] As shown in Figure 5a, the H_2UO molecule is bending toward one side with a half-naked U(IV) atom, which facilitates weak U—Ar interactions on the other side. Indeed, our preliminary calculations on $H_2UO(Ar)_n$ species (n = 1, 2, 3) indicate

(50) Li, J.; Bursten, B. E.; Liang, B.; Andrews, L. *Science* **2002**, *295*, 2242.
(51) Li, J.; Bursten, B. E.; Andrews, L.; Marsden, C. J. *J. Am. Chem. Soc.* **2004**, *126*, 3424.
(52) Wang, X.; Andrews, L.; Li, J.; Bursten, B. E. *Angew. Chem., Int. Ed.* **2004**, *43*, 2554.

that the optimized U···Ar distances are ~3.49 Å, and the U═O and U—H distances increase about 0.001 Å upon addition of each Ar atom. The U···Ar binding energy is about 1 kcal/mol per Ar atom. As expected for a low-valent U atom, the binding energies of the Ar atoms to the U(IV) atom are indeed very small, indicating that the Ar—U(IV) interaction is within a normal polarizability-based matrix effect. However, these results indicate that the binding of Ar atoms to the U atom of H_2UO will help to reduce the vibrational frequencies and to stabilize these otherwise unstable species. Consistent with these results, the experimental spectra indeed show matrix site effects, with a 864.8 cm^{-1} band near the 859.4 cm^{-1} band, which is presumably due to the $H_2UO(Ar)_n$ species with a different coordination number of Ar atoms. This 864.8 cm^{-1} band has similar isotopic shifts and mixed isotopic splitting patterns in the isotopic-substituted samples as compared to the 859.4 cm^{-1} band. However, it increased on irradiation but decreased on annealing. These observations indicate that H_2UO could be formed via a photoinduced reaction between a uranium atom and a water molecule in the matrix cage. The so-formed H_2UO molecule may exhibit a slightly different Ar coordination number (i.e. a different matrix cage) and relax to a more stable form upon annealing the matrix (Figure 1). The initial absorption observed at 864.8 cm^{-1} after deposition is also due to the same mechanism, since the laser plume provides an efficient photolysis source. Two more bands at 1442.7 and 1396.3 cm^{-1} tracked with the 864.8 cm^{-1} band and are due to the symmetric and antisymmetric H—U—H stretching modes.

2. HUO(OH). The band observed on deposition at 834.3 cm^{-1} increased by half on 25 K annealing. The band decreased by a quarter on full-arc irradiation and markedly increased on the following 35 K annealing. This band has a signature U═O vibration ^{18}O red-shift to 789.9 cm^{-1}, with an $^{16}O/^{18}O$ isotopic frequency ratio of 1.0562. In the D_2O experiment, the band red-shifted to 832.3 cm^{-1}. In both mixed isotopic experiments ($^{16}O/^{18}O$ and H/D), only doublets were observed. The band is appropriate for a U═O vibrational mode perturbed by one H atom. The 1370.5 cm^{-1} band, also observed on deposition, tracked with the 834.3 cm^{-1} band throughout the annealing and photoirradiation cycles. This band showed a very small 0.2 cm^{-1} shift in the $H_2{}^{18}O$ experiment and red-shifted to 982.7 cm^{-1} in the D_2O experiment, which indicates that this band is a U—H vibration with very little oxygen perturbation. A third band at 575.7 cm^{-1} tracked with the 834.3 and 1370.5 cm^{-1} bands; this region is appropriate for a U—OH vibration. The band red-shifted to 556.8 cm^{-1} in the D_2O experiment; however, the ^{18}O counterpart was too weak to be observed. This band showed a doublet in the mixed H/D experiment. Similar to the HThO(OH) molecule,[24] a HUO(OH) molecule is hence identified based on the observation of three modes. This molecule has another infrared mode, namely the O—H stretch; however, very strong H_2O absorption dominated the spectral region around 3800 cm^{-1}, and we cannot definitively identify this mode.

The DFT calculation on HUO(OH) finds a C_1 symmetry, pyramidal, triplet ground state for this U(IV) species (Figure 5b). The calculated geometric parameters are listed in Table 2. The vibrational analysis on this ground-state geometry predicts U—H, U═O, and U—OH vibrational modes at 1457, 854, and 625 cm^{-1}, which need to be scaled down by 0.941, 0.977, and 0.921, respectively, to fit the experimental frequencies for the matrix species. The isotopic frequencies, listed in Table 2, fit with the experimental results reasonably well. We might expect that the pyramidal HUO(OH) molecule will also be subject to weak U—Ar interactions, and we have modeled such interactions computationally. With one Ar atom included in the coordination shell, the U—Ar distance is found to be 3.48 Å and the U—Ar binding energy is again about 1 kcal/mol. The U—O and U—H distances are slightly decreased. With the inclusion of more Ar atoms in the coordination shell for modeling the matrix effect, the U—O and U—H distances are expected to be decreased further and the theoretical vibrational frequencies are expected to be in somewhat better agreement with the experimental values.

3. H_2UO_2. A sharp band at 885.9 cm^{-1} was observed on deposition. This band decreased on annealing and then markedly increased on irradiation. In the D_2O experiment, this band red-shifted slightly, but definitively, to 885.2 cm^{-1}. In the $H_2{}^{18}O$ experiment, the band shifted to 842.0 cm^{-1} with an $^{16}O/^{18}O$ frequency ratio of 1.0521. This isotopic ratio is considerably smaller than that of a UO vibration; however, it is close to the $^{16}O/^{18}O$ ratio of 1.0529 for the antisymmetric U—O stretching mode of UO_2. In the mixed $^{16}O/^{18}O$ experiment, the 885.9 cm^{-1} band gave a triplet feature with a new intermediate band at 871.8 cm^{-1} (Figure 4), which indicates that two equivalent O atoms participate in this vibration. The asymmetry in the triplet points to a lower frequency symmetric stretching mode, which is too weak (and too low based on our calculations) to be observed here. It is obvious that the 885.9 cm^{-1} band is a H-perturbed antisymmetric UO_2 vibrational mode. In the mixed H/D experiment, the isotopic splitting pattern cannot be resolved. However, in the U—H vibrational region, a 1406.4 cm^{-1} band tracked with the 885.9 cm^{-1} band. This band red-shifted to 1006.0 cm^{-1} in the D_2O experiment, whereas very little shift was observed in the $H_2{}^{18}O$ investigations. In the mixed $H_2O + HDO + D_2O$ experiment, a new band observed at 1019.7 cm^{-1} tracked with the 1006.0 and 885.9 cm^{-1} bands and was stronger than the 1006.0 cm^{-1} band (Figure 3). Similar to the UH_2 vibrations in the H_2UO molecule discussed earlier, this new clearly mixed H/D isotopic band at 1019.7 cm^{-1} is the U—D vibration in a H—U—D unit. In contrast to the case of H_2UO, only one UH_2 vibration is observed. The 1406.4 cm^{-1} band is due to an antisymmetric UH_2 vibration, where the symmetric mode is not observed. Overall, the H_2UO_2 molecule is identified, and the two bands at 1406.4 and 885.9 cm^{-1} are assigned to antisymmetric UH_2 and UO_2 stretching modes, respectively.

The H_2UO_2 molecule is interesting for several reasons. First, it is formally a U(VI) complex. Therefore, unlike the U(IV) species discussed earlier, it is not a species with an analogue in our previous studies of the reactions of Th with H_2O.[24] Second, H_2UO_2 can be considered a complex of the

ubiquitous uranyl ion, UO_2^{2+}, with two H^- "ligands." As such, it represents the simplest possible neutral complex of the uranyl ion. The uranyl ion has a strong preference for a linear structure, both as a naked ion and in the presence of neutral and anionic ligands.[53] The structures of UO_2X_2 complexes have been the subject of several recent theoretical studies, with some disagreement as to whether a planar (D_{2h}) or nonplanar (C_{2v}) structure is preferred.[54] Finally, H_2UO_2 is analogous to UO_2F_2, which has been prepared by the hydrolysis of UF_6 and by the reaction of laser-ablated U atoms with $Ar/O_2/F_2$ mixtures.[55,56] The OUO stretching frequency (939.6 cm^{-1}) is slightly higher for UO_2F_2. We were therefore particularly interested in determining the structure and calculated frequencies of the H_2UO_2 molecule.

The DFT calculation on H_2UO_2 was initially started from a C_{2v} structure, but the calculated vibrational spectrum does not agree with the experimental values. The geometry optimizations were then performed on a planar structure with D_{2h} symmetry, as shown in Figure 5c. The ^1A_g ground state of the planar H_2UO_2 molecule is energetically very close to the C_{2v} structure, and they both have all real frequencies at the PW91 level of theory. The D_{2h} structure is 16 kcal/mol lower in energy than the HUO(OH) isomer (Figure 5b), and the bond lengths for U—H and U═O are 2.009 and 1.796 Å, respectively. Infrared active antisymmetric UH_2 and UO_2 modes were predicted at 1408 and 943 cm^{-1}; relative to the experimental values, the antisymmetric UH_2 mode is overestimated by 2 cm^{-1}, while the UO_2 mode is overestimated by 57 cm^{-1}.

Because the planar structure of H_2UO_2 provides open coordination sites on both sides of the molecular plane and the U atom is in the VI oxidation state, it is interesting to explore how the U atom could interact with the Ar atoms in the matrix. We performed geometry optimizations of the $H_2UO_2(Ar)_n$ species with $n = 1-5$, and the binding energy curve for the process $H_2UO_2 + nAr \rightarrow H_2UO_2(Ar)_n$ is shown in Figure 6. It is found that the H_2UO_2 molecule can interact with Ar atoms quite effectively, with the U−Ar distance being 3.14 and 3.17 Å for $H_2UO_2(Ar)$ and $H_2UO_2(Ar)_2$, respectively. The binding energies for the coordination of the first and second Ar atoms are 2.9 and 2.7 kcal/mol, close to those found for $CUO(Ar)_n$.[57] The binding energy increases as the number of coordinated Ar atoms increases from 1 to 4 and begins to decrease when 5 Ar atoms are coordinated. The binding energies of 3 and 4 Ar atoms with H_2UO_2 are sufficiently close to each other that a preferred coordination number of Ar ligands to H_2UO_2 cannot be determined at the current level of theory. In addition, the present calculations

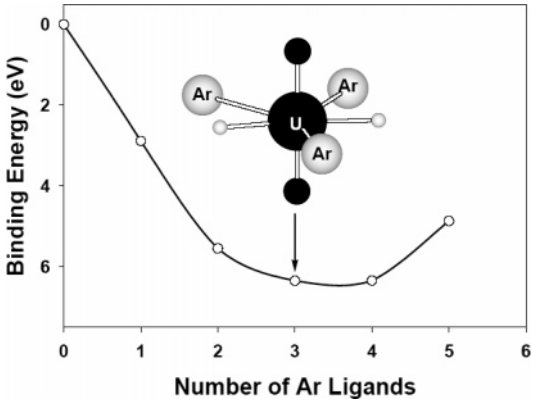

Figure 6. Binding energy curve for the process $H_2UO_2 + nAr \rightarrow H_2UO_2(Ar)_n$. The inset shows the optimized structure of $H_2UO_2(Ar)_3$.

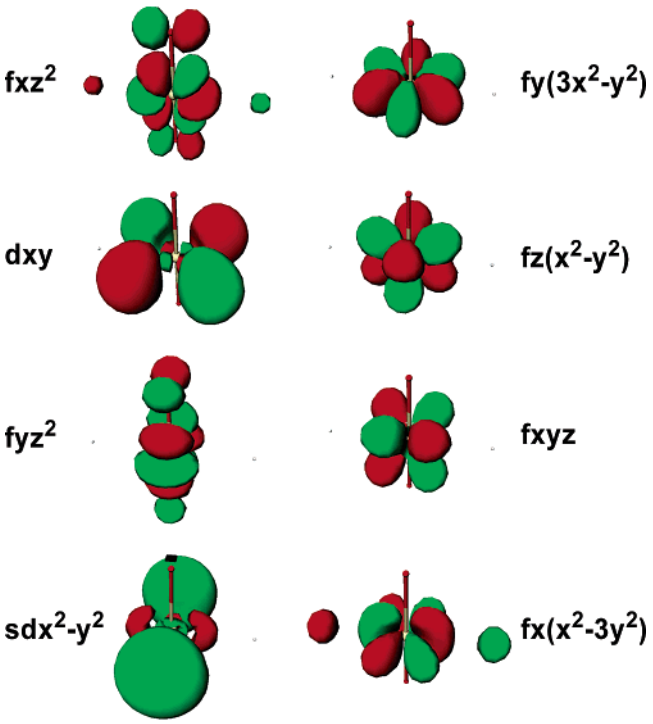

Figure 7. Three-dimensional contour surfaces of eight low-lying unoccupied molecular orbitals in the H_2UO_2 molecule. The orbital contours are set as 0.06 throughout.

did not include in the basis sets the diffuse functions, which are expected to increase the U—Ar binding energies and stretching frequencies. Our calculations show that the fully symmetric stretching frequencies of U—Ar are 55 and 75 cm^{-1} for $H_2UO_2(Ar)_3$ and 38 and 57 cm^{-1} for $H_2UO_2(Ar)_4$.

Figure 7 shows the three-dimensional contours of the eight low-lying unoccupied molecular orbitals of H_2UO_2, which represent the six 5f orbitals and two 6d orbitals of U atoms. As is shown, the U 6d orbitals are significantly more diffuse than the 5f orbitals and thus can interact more strongly with incoming ligands. The other MOs are energetically much higher in energy than these orbitals. Because of the large electronegativity of the oxo ligands, there is significant charge transfer from U to the ligands, as shown by the Mulliken net charges: U (+1.74), O (−0.57), and H (−0.30). The two low-lying U 6d orbitals can accept electron donation from the lone pairs of the weak Lewis base Ar, which forms

(53) See, for example: (a) Pepper, M.; Bursten, B. E. *Chem. Rev.* **1991**, *91*, 719. (b) Denning, R. G. *Struct. Bonding (Berlin)* **1992**, *79*, 215.
(54) See, for example: (a) Wang, Q.; Pitzer, R. M. *J. Phys. Chem. A* **2001**, *105*, 8370. (b) Straka, M.; Dyall, K. G.; Pyykko, P. *Theor. Chim. Acta* **2001**, *106*, 393. (c) Clavaguera-Sarrio, C.; Hoyau, S.; Ismail, N.; Marsden, C. J. *J. Phys. Chem. A* **2003**, *107*, 4515. (d) Schimmelpfennig, B.; Privalov, T.; Wahlgren, U.; Grenthe, I. *J. Phys. Chem. A* **2003**, *107*, 9705.
(55) Sherrow, S. A.; Hunt, R. D. *J. Phys. Chem.* **1992**, *96*, 1095.
(56) Souter, P. F.; Andrews, L. *J. Mol. Struct.* **1997**, *412*, 161.
(57) Bursten, B. E.; Drummond, M. L.; Li, J. *Faraday Discuss*. **2003**, *124*, 1.

the weak U—Ar bonding. This is exactly the same type of Lewis acid—base interaction between the U and Ar atoms on the $CUO(Ar)_n$ species.[50] When three Ar atoms are coordinated, the UH_2 and UO_2 modes are changed from 1408 and 943 cm^{-1} to 1396 and 937 cm^{-1}, respectively.

4. $H_2UO(OH)_2$. A weak band at 845.3 cm^{-1} on deposition increased considerably on annealing, disappeared on irradiation, and then reappeared after annealing to 35 K. This band showed very little deuterium shift, but it shifted to 800.2 cm^{-1} in the $H_2{}^{18}O$ experiment, with a signature $^{16}O/^{18}O$ frequency ratio of 1.0564. The 845.3 cm^{-1} band exhibited a doublet with two pure isotopic bands in the mixed $H_2{}^{16}O + H_2{}^{18}O$ experiment, which characterizes a single U═O bond stretching mode. The $H_2O + HDO + D_2O$ experiment gave a broader band centered at 845.2 cm^{-1}, which shows that more than one hydrogen is involved. The 845.3 cm^{-1} band is clearly a U═O stretching mode. An associated band at 1352.4 cm^{-1} in the U—H vibrational region red-shifted to 966.6 cm^{-1} in the D_2O experiment, which identifies a U—H vibration. In the mixed H/D experiment, no additional bands can be clearly identified in the U—H and U—D stretching region. A third associated band was observed at 591.2 cm^{-1}. This band shifted to 566.2 and 567.3 cm^{-1} in the $H_2{}^{18}O$ and D_2O experiments, respectively. In the mixed H/D experiment, the band showed a triplet splitting pattern with a new band in the middle of two pure isotopic bands at 574.4 cm^{-1} (Figure 3). Hence, the 591.2 cm^{-1} band is assigned to an antisymmetric U—$(OH)_2$ vibrational mode.

Considering all three observed modes and six total valence electrons for uranium, a responsible molecule is $H_nUO(OH)_2$ with $n = 1$ or 2. The first thought on this molecule is $HUO(OH)_2$, because only one U—H mode is observed, and no additional band is observed in the mixed H/D experiment. However, the other mode could be infrared inactive, and H—U—D vibrations might be covered by other stronger absorptions. To clarify the number of hydrogen atoms, we measured the integrated areas of the U—D [more precisely, the U—D_n ($n = 1$ or 2) vibration] and U═O stretching bands in the D_2O and mixed $H_2O + HDO + D_2O$ experiments. In the D_2O experiment after 30 K annealing (Figure 2b), the integrated areas of the 966.6 cm^{-1} (U—D) and 845.1 cm^{-1} (U═O) bands are 0.0456 and 0.0100 AU cm^{-1}, respectively, whereas, in the mixed H/D experiment after 30 K annealing (Figure 3b), the integrated areas of the same bands are 0.0038 and 0.0057 AU cm^{-1}, respectively. The intensity ratios between the U—D/U═O bands in the D_2O and HDO experiments are 4.56 and 0.67, respectively; therefore, the ratio ("*R*" value for convenience) of these ratios in the D_2O and HDO experiments is 6.8. Taking the H/D ratio of 1.5:1 in the mixed H/D experiment into account, the expected *R* value for a HUO_n-type molecule would be 2.5, whereas, for a H_2UO_n-type molecule, the *R* value would be $(2.5)^2 = 6.3$. In the same experiment (Figures 2b and 3b), we calculated the *R* values for the HUO(OH), H_2UO, and H_2UO_2 molecules as 2.0, 7.2, and 5.5, respectively. The 966.6 cm^{-1} band is hence assigned to the antisymmetric DUD stretching mode. Overall, a possible $H_2UO(OH)_2$ molecule is tentatively identified, and three bands at 1352.3, 845.3, and 591.2 cm^{-1} are assigned to the antisymmetric UH_2, U═O, and antisymmetric U—$(OH)_2$ modes, respectively.

Similar to H_2UO_2, $H_2UO(OH)_2$ is another U(VI) compound. Even though the assignment of the experimental bands to $H_2UO(OH)_2$ is rather tenuous, we thought that this molecule was interesting enough that we did perform DFT calculations on it to determine its likely structure and predicted vibrational frequencies. The DFT calculations on this complicated molecule were performed first on a C_{2v} geometry; however, the C_{2v} structure is a transition state with an imaginary frequency of 98 cm^{-1}. The C_{2v} structure is more than 2 kcal/mol higher in energy than the C_s structures. In two lower energy C_s structures, the three oxygen atoms and the uranium atom are almost in the same plane, while two uranium-bonded hydrogen atoms adopt different conformations. In one form, two hydrogen atoms are adjacent, and both are on one side of the UO_3 plane; however, this structure is still 12 kcal/mol higher in energy than the other C_s structure, in which the two uranium-bonded hydrogen atoms are on opposite sides of the UO_3 plane. The latter is the lowest energy structure of the $H_2UO(OH)_2$ molecule (Figure 5d), which has a $^1A'$ ground state. In this structure, O═U$(OH)_2$ is in one plane, which acts as the symmetry plane in this molecule. The two OH groups are not symmetric, which precludes a higher symmetry C_{2v} structure. The vibrational analysis on the $^1A'$ ground state predicts three strong modes at 1445, 869, and 637 cm^{-1}, which require scale factors 0.936, 0.973, and 0.928, respectively. The computed isotopic frequencies, listed in Table 2, seem appropriate for the experimental values. On the basis of the DFT calculations, we cannot say with certainty that $H_2UO(OH)_2$ has been produced in the matrix, although the theoretical results are in reasonable accord with the experimental observations.

5. Other Absorptions. Bands observed at 1308.2 and 796.5 cm^{-1} on deposition (labeled X) changed little during initial annealing and irradiation but decreased after the final annealing to 35 K. In the $H_2{}^{18}O$ experiment, the 796.5 cm^{-1} band shifted to 753.2 cm^{-1}, a typical U═O stretching mode shift with a $^{16}O/^{18}O$ isotopic frequency ratio of 1.0575. In the D_2O experiment, the 1308.2 cm^{-1} band decreased to 932.5 cm^{-1}, and the lower band decreased to 795.4 cm^{-1}. These two bands are probably the U—H and U═O stretching modes in a new molecule. In the mixed $H_2O + HDO + D_2O$ experiment, no intermediate components were observed; a doublet was almost resolved for the lower band. In the mixed $H_2{}^{16}O + H_2{}^{18}O$ experiment, the lower band gave a doublet, which suggests that only one O atom is involved. A possible assignment is to the HUO molecule; however, the theoretical results on this U(III) complex do not fit as well as we would like, but high multiplicity states are clearly more difficult to calculate accurately.

Our DFT calculations on HUO predict a bent C_s molecule with a $^4A''$ ground state and an f^3 $[(a')^1(a'')^1(a')^1]$ configuration. The U—H and U═O bond lengths are 1.823 and 1.992 Å, and ∠HUO is 105.6°. The vibrational analyses produced U—H and U═O stretching modes at 1443 and 862 cm^{-1}, with absorption intensities of 389 and 218 km/mol. The 1308.2 and 796.5 cm^{-1} bands are clearly due to a molecule

containing U—H and U═O functional groups, and we tentatively assign these bands to HUO.

A weak band at 570.5 cm^{-1} (denoted "X" in Figures 1−3) was observed on deposition and increased on annealing. In the D_2O experiment, this band shifted to 551.8 cm^{-1}, but the $H_2{}^{18}O$ counterpart was too weak to be observed. The band showed a triplet splitting pattern in the mixed H/D experiment, which is appropriate for a U—$(OH)_2$ stretching mode in a compound with a $U(OH)_2$ group.

B. U + H_2/O_2. Reactions were performed with H_2/O_2 mixtures using similar laser power and gas flow rate. The product bands include strong UO and UO_2 absorptions and relatively strong UH, UH_2, UH_3, UH_4, and U_2H_2 bands.[23,46,47] Also observed are HO_2 and Ar_nH^+ absorptions.[48,49] Reaction products involving both oxygen and hydrogen atoms include strong absorptions for H_2UO_2 at 1406.4 and 885.9 cm^{-1} and the X bands at 1308.2 and 796.5 cm^{-1}. A weak HUO(OH) band was observed at 834.3 cm^{-1} after 30 K annealing. The H_2UO product was not observed in the H_2/O_2 investigations, which means that H_2UO is not made from the elements but is formed by rearrangement of the primary U + H_2O reaction product.

IV. Reaction Mechanisms

The mechanisms of formation for primary reaction products are illustrated below:

$$U + H_2O \rightarrow [HU(OH)]^* \rightarrow HU(OH) \quad (1)$$

$$U + H_2O \rightarrow [HU(OH)]^* \rightarrow H_2UO \quad (2)$$

$$U + H_2O \rightarrow H_2 + UO \quad (3)$$

$$UO + H_2 \rightarrow H_2UO \quad (4)$$

The initial reaction between energetic laser-ablated uranium atoms and H_2O is possible through reaction 1 which forms the intermediate [HU(OH)]*. The highly excited [HU(OH)]* may be quenched by collision with the matrix gas; however, no evidence for this product was found, which attests the instability of divalent uranium. The main pathways for relaxation of [HU(OH)]* are through channels 2 and 3, either by rearranging to the more stable H_2UO isomer or by eliminating hydrogen to form UO. There is tentative experimental evidence for isolated HUO. Both reactions 2 and 4 can, in principle, produce H_2UO. We believe that reaction 4 is not the mechanism in this investigation, since H_2UO is not observed in our U + H_2/O_2 experiment. On the other hand, the H_2UO bands increased markedly upon annealing with U and H_2O, and reaction 2 may involve the [HU(OH)]* intermediate, followed by fast rearrangement.

In the laser-ablation process, excited U atoms can form UO after elimination of hydrogen (reaction 3). Further reaction with H_2O forms UO_2. In the matrix, another reaction between UO and H_2O, eq 5, enters the competition:

$$UO + H_2O \rightarrow HUO(OH) \quad (5)$$

In the matrix-annealing cycles, this insertion reaction is favored over the elimination of hydrogen atoms, since the HUO(OH) absorptions increased considerably whereas the UO_2 absorption showed little change. Furthermore, HUO(OH) may undergo isomerization to form the more stable H_2UO_2 molecule:

$$HUO(OH) \rightarrow H_2UO_2 \quad (\Delta E = -15 \text{ kcal/mol}) \quad (6)$$

Although this reaction is thermodynamically favored by 15 kcal/mol, reaction 6 apparently has a high barrier: first, the geometrical reorientation is tremendous in this process and may involve a high-energy, three-member-ring (U—O—H) transition state; second, in our experiments, the H_2UO_2 absorptions only increased on irradiation when HUO(OH) decreased. However, in the experiment with U + H_2/O_2, a large yield of H_2UO_2 was observed with no H_2UO, and HUO(OH) was detected on annealing. The formation of H_2UO_2 from H_2/O_2 must proceed in different pathways such as reaction between UH_2 and O_2 or reaction between UO_2 and H_2, although our observations cannot determine which process is favored.

Two reactions can, in principle, form $H_2UO(OH)_2$:

$$HUO(OH) + H_2O \rightarrow H_2UO(OH)_2 \quad (7)$$

$$H_2UO_2 + H_2O \leftrightarrow H_2UO(OH)_2 \quad (8)$$

Reaction 7 is similar to reaction 5, which involves a direct insertion into H_2O. Reaction 8 may involve a four-member-ring transition state in which one U═O bond in H_2UO_2 interacts with one O—H bond in H_2O. The electropositive U atom forms a new bond with the electronegative O atom in H_2O, while the oxygen in the U═O bond H-bonds with the H atom in H_2O. As a result, two OH groups replace the previous U═O bond in H_2UO_2 to form $H_2UO(OH)_2$. A similar four-member-ring transition state has been reported recently in a theoretical study of the hydrolysis of CrO_3.[58] During irradiation, the H_2UO_2 absorptions increased whereas the $H_2UO(OH)_2$ bands decreased, suggesting the reverse of reaction 8 might also happen.

V. Conclusions

Laser-ablated U atoms react with H_2O during condensation in excess argon. On the basis of isotopic substitution, infrared absorptions at 1416.3, 1377.1, and 859.4 cm^{-1} are assigned to symmetric H—U—H, antisymmetric H—U—H, and U═O stretching vibrations of the stable primary product, H_2UO isomer. Uranium monoxide (UO) produced in the reaction inserts into H_2O to form HUO(OH), which absorbs at 1370.5, 834.3, and 575.7 cm^{-1}. HUO(OH) can undergo photoinduced isomerization to form a more stable H_2UO_2 molecule, which absorbs at 1406.4 and 885.9 cm^{-1}. Addition of another water molecule to either HUO(OH) or H_2UO_2 produces a complex that has been tentatively assigned as $H_2UO(OH)_2$. Relativistic DFT calculations were performed on all proposed molecules and some other possible isomers. Relatively good agreement between experimental and calculated vibrational frequencies,

(58) Johnson, J. R. T.; Panas, I. *Inorg. Chem.* **2000**, *39*, 3181.

relative absorption intensities, and isotopic shifts supports the infrared absorption assignments.

These species, particularly the H_2UO_2 molecule, tend to form weak Ar-coordinated complexes. It is necessary to include the Ar matrix effects for these species in order to provide more quantitative agreement between theoretical calculations and the matrix infrared frequencies. Application of a higher level of electron correlation theory and better basis sets to these problems would be interesting, but it is beyond our scope in this paper.

The reactions of laser-ablated U atoms provide interesting similarities and contrasts to those observed for Th atoms.[24] For oxidation states of +4 or lower, the chemistry of U parallels that of Th in the formation of species such as H_2AnO and HAn(O)OH. This mutual aspect of Th and U chemistry is largely driven by the high oxophilicity of the early actinide elements. As shown here, the U chemistry progresses into oxidation states higher than can be achieved by Th, especially in the formation of the U(VI) complexes H_2UO_2 and possibly $H_2UO(OH)_2$. We believe that some of the new molecules reported here, especially the U(VI) complexes that have uranium in its highest possible oxidation state, may be involved in the oxidation of uranium in aqueous systems, which is an important issue in nuclear waste remediation.

Acknowledgment. The authors gratefully acknowledge support from the National Science Foundation (Grant CHE 00-78836 to L.A.) and the Department of Energy (Grant DE-FG02-01ER15135 to B.E.B). This research was performed in part using the Molecular Science Computing Facility (MSCF) in the William R. Wiley Environmental Molecular Sciences Laboratory, a national scientific user facility sponsored by the U.S. Department of Energy's Office of Biological and Environmental Research and located at the Pacific Northwest National Laboratory. Pacific Northwest is operated for the Department of Energy by Battelle.

IC0483951